

Evaluation of the Collapse Susceptibility of the Northern Foot of the Tianshan Mountains

Zhenya Chen¹, Jie Tang¹, Wei Huang¹, Baoying Ye^{2*}

¹No. 1 Regional Geological Survey Team, Xinjiang Bureau of Geo-Exploration and Mineral Development, Urumqi, China

²School of Land Science and Technology, China University of Geosciences (Beijing), Beijing, China

Email: 619534449@qq.com, *yebaoying@cugb.edu.cn

How to cite this paper: Chen, Z. Y., Tang, J., Huang, W., & Ye, B. Y. (2022). Evaluation of the Collapse Susceptibility of the Northern Foot of the Tianshan Mountains. *Journal of Geoscience and Environment Protection*, 10, 318-327.
<https://doi.org/10.4236/gep.2022.104020>

Received: April 11, 2022

Accepted: April 26, 2022

Published: April 29, 2022

Abstract

Collapse is a geological disaster second only to landslides and occurs in large numbers every year in the northern foothills of the Tianshan Mountains in Xinjiang, China. We collected a variety of data such as topography, geological vegetation coverage, and human activities, and used spatial correlation analysis to eliminate factors with strong correlations. The frequency of collapse was calculated by the frequency ratio method and a hierarchical map was made. The result shows, in low susceptibility zone (LSI = 0 - 4), only 3 collapses happened, and 0.39% of total collapses. In middle susceptibility zone (LSI = 4 - 7.5), 35 collapses happened, and 5.66% of total collapses. In high susceptibility zone (LSI = 7.5 - 10), 64 collapses happened, and 10.36% of total collapses. In extremely high susceptibility zone (LSI = 10 - 14), 516 collapses happened, and 83.5% of total collapses. Using the GIS-based frequency method, the susceptibility to collapse was calculated and mapped, which was in good agreement with the actual landslide data. Collapse susceptibility results provide guidance for engineering construction.

Keywords

Tianshan Mountain, Collapse, Susceptibility, Frequency Ratio

1. Introduction

In 2021, a total of 4727 geological disasters will occur in China, causing 70 deaths and direct economic losses of 3,158,050,100 yuan RMB. In terms of disaster types, there were 2320 landslides, 1733 collapses, 369 debris flows, 274 ground subsidence, 21 ground fissures, and 10 ground subsidence, with collapse accounting for 36.7% of the total (data from Ministry of Natural Resources of the People's

*Corresponding author.

Republic of China, <http://www.mnr.gov.cn/>). The bedrock on the northern slope of the Tianshan Mountains is exposed, and faults and structural joints are developed, forming the basic conditions for collapse. The temperature difference between day and night is large, and the precipitation infiltrates along the joints and fissures, causing the rocks to freeze and crack into blocks. It is an area prone to collapse disasters.

Evaluating the susceptibility of geological hazards and setting up warning areas are important tasks to reduce losses. There have been many studies carried out evaluation of collapse susceptibility using GIS with the assessment model such as statistical model (Van Den Eeckhaut M., et al., 2012; He Shuangshuang et al., 2019), artificial neural network (Poudyal C.P. et al., 2010; Polykretis et al., 2018; Bragganolo L. et al., 2020), support vector machine (Li Y. et al., 2020), random forest model (Shi Hui et al., 2021), machine learning (Huang F. et al., 2020), logistic regression model (Xu Xianghua, 2010; Fang Miao et al., 2011; Xing X.F. et al., 2021).

In the study, the frequency ratio model (Lee et al., 2006; Li Langping et al., 2017; Li Wenyan, 2020) was used to evaluate the collapse susceptibility in the northern foot of the Tianshan Mountains. The frequency ratio (FR) model is a well accepted and popular quantitative approach for the preparation of collapse susceptibility maps (Lee & Talib, 2005; Intarawichian et al., 2011). Most of the work was done using ArcGIS software, which was used for spatial process and mapping. Python with ArcPy module and Hydrological tools intergraded in ArcGIS finished data batching process and Watershed Hydrological Analysis.

2. Materials

2.1. Description of Study Area

The study area is located in the northern part of the Tianshan Mountains, including Changji City, Hutubi County, Manas County, and Wusu City. The geographic coordinates are between 84° 18' - 87° 18' longitude and 43° 18' - 44° 12' latitude (**Figure 1**), and the study area covers 3660.9 km².

The study area is located at the northern foot of Xinjiang and the southern margin of the Junggar Basin. The terrain is generally high in the south and low in the north, high in the east and low in the west, and slopes from southeast to northwest. The south is the middle and high mountains, which is about 4000 - 5000 m, and the highest peak, Heyuan Peak, is 5289 m; the northern part is a desert area, with an altitude of about 370 - 500 m. The northwestern part is a fine soil plain and the edge of the desert, and the lowest point is 280 m. It is a typical continental arid and semi-arid climate, with an average annual temperature of 6.8°C. The average temperature in July is 24°C - 28°C, and the average temperature in January is -10°C - 20°C. The average annual precipitation is 167.2 - 220 mm, and the average annual evaporation is about 400 - 1088.2 mm.

There are a total of 618 collapse points in the study area, and the collapse is mainly distributed in the low mountain area where erosion and denudation are involved and the middle mountain area where the fault block rises and is moderately

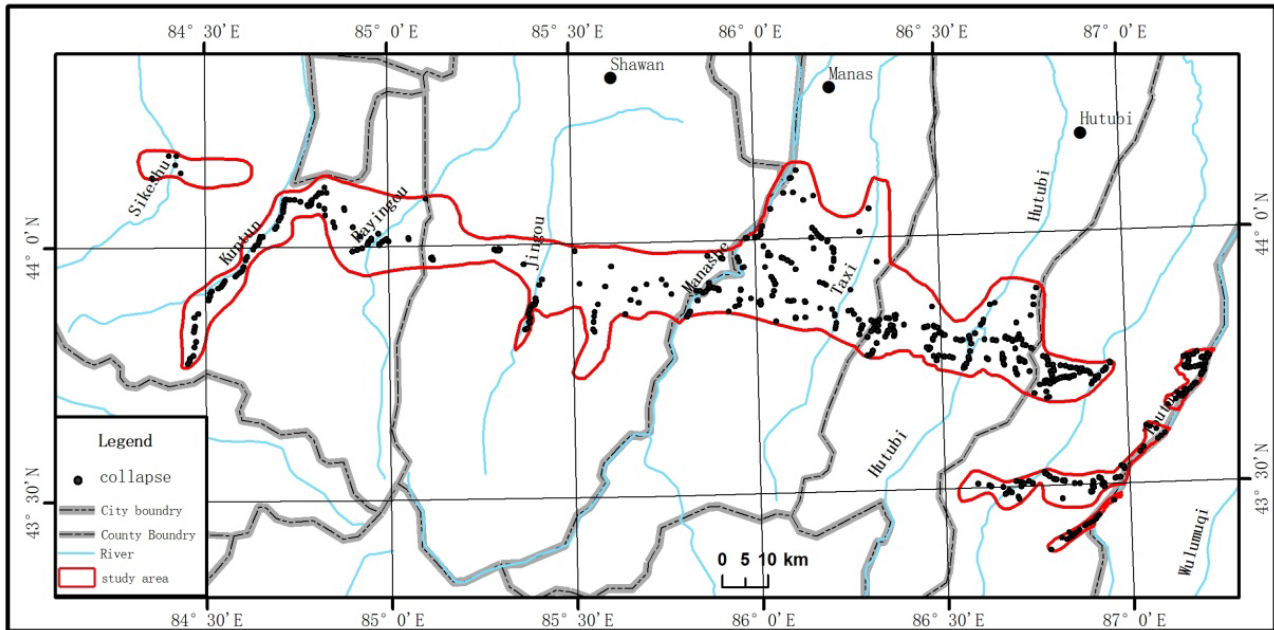


Figure 1. Location of study area.

cut. In addition, in the upper reaches of the Bayingou River Basin, the Bayingou river Pasture in Wusu City and the middle and upper reaches of the Kuitun River Basin are densely distributed along the Duku highway. Rock collapse mainly threatens the surrounding township residents, livestock, township roads, No.101 provincial highway, water conservancy facilities, etc.

2.2. Data and Method

2.2.1. Data

The factors that affect the collapse include terrain slope, including slope, aspect, and relief, and geological factors include lithology, faults, vegetation coverage, and human activities. In this paper, we collect data related to collapses (**Table 1**).

The collapse disaster point data comes from the document data of the field survey. Terrain data from USGS SRTM (Tom G. Farr et al., 2007). Slope, aspect, water system and relief maps were data is derived from SRTM DEM. lithology and fault map were from Regional Geological Survey Map of 1:50,000. Road map is from Gaode digital Map (2020). Landuse data is from database of China 2nd National Land and Resources Survey (2018). Vegetation index is calculated from Landsat 8 remote sensing data of 2020.

The following factors are formed: slope, aspect, relief, distance to drainage network, drainage network density, lithology, distance to fault, vegetation coverage, landuse, distance to road. All the data were processed in ArcGIS 10.1.

2.2.2. Correlation Analysis

In order to judge the correlation between the disaster-pregnant factors, the correlation coefficient ($Corr_{ij}$) can be used to represent the correlation between the two. The formula is as follows:

Table 1. Data of study area.

| Classification | scale | Data type | Data source |
|------------------|----------|-----------|---|
| Collapse hazard | 1:10,000 | Point | Field Survey |
| Topological map | 30 m | GRID | SRTM |
| Slope map | 30 m | GRID | From SRTM |
| Aspect map | 30 m | GRID | From SRTM |
| Water system map | | line | From SRTM |
| Terrain relief | | GRID | From SRTM |
| Fault map | 1:50,000 | line | from geological map |
| lithology | 1:50,000 | polygon | from geological map |
| Land use map | 1:10,000 | polygon | China 2 nd National Land and Resources Survey (2018) |
| Road map | 1:50,000 | Line | Gaode digital Map(2020) |
| Vegetation Index | 30 m | GRID | From landsat NDVI (2020) |

$$Corr_{ij} = \frac{Cov_{ij}}{\delta_i \delta_j} \quad (1)$$

$$Cov_{ij} = \frac{\sum_{k=1}^N (Z_{ik} - u_i)(Z_{jk} - u_j)}{N - 1} \quad (2)$$

where, Cov_{ij} , covariance matrix, are the covariances between all pairs of factors, Z , value of a cell, I, j are factors, μ is the mean of factors, N is the number of cells, k denotes a particular cell. δ is standard deviation of factors i and j .

The value of C ranges from -1 to 1 . $C = 1$ means that the two raster images are completely correlated, and $C = 0$ means that the two raster images have no correlation. $C = -1$ means that the two raster images are negatively correlated.

2.2.3. Frequency Ratio Method

The formation of geological disasters is affected by a variety of factors, and the frequency ratio method reflects the combination of the most hazard-prone factors and their subdivisions in a certain geological environment; specifically, the frequency and region of geological disasters under the action of a certain factor in a specific evaluation unit. The frequency of geological disasters can be compared. Corresponding to a certain factor, the information quantity formula of geological disasters under a specific state can be expressed as:

$$Fri = \frac{N_i/N}{S_i/S} \quad (3)$$

where, Fri is the frequency of rock collapse corresponding to a specific factor in i domain, N_i is the rock collapse area or the number of collapse points corresponding to specific factors in i domain, S_i is the distribution area corresponding to a specific factor in i internal, N is the total collapse area or the total number of

collapse points in the survey area, S is the total area of the survey area.

Since each evaluation unit is affected by many factors, and each factor has several states (domain), the total frequency of collapse under the combined conditions of each state factor can be determined by the following formula:

$$LSI = \sum_i^n \frac{N_i/N}{S_i/S} \quad (4)$$

LSI is the total frequency of collapse under various factors in a specific unit, indicating the possibility of collapse, which can be used as a collapse susceptibility index.

According to the calculated LSI value interval and the actual situation of the collapse, the collapse susceptibility of the study area is divided into four grades: extremely high, high, medium and low.

3. Results

3.1. Correlation Coefficient

In ArcGIS, the rock collapse-pregnant factor layers are grouped into stacks (makestack command), and then the correlation coefficient between layers is calculated (stackstats command). The correlation coefficient matrix of disaster-pregnant factors is obtained (Table 2). The data shows that the correlation between slope and terrain fluctuation is very high, and the correlation coefficient $c = 0.8858$. Therefore, one of the two should be eliminated, and we will eliminate the fluctuation factor. The correlation between the remaining factors is very low, and the largest correlation coefficient (c) is the distance between the road and the water system, $c = 0.02438$.

Through correlation analysis, the disaster-pregnant factors are determined as

Table 2. The relation of rock collapse-pregnant factors.

| | X1 | X2 | X3 | X4 | X5 | X6 | X7 | X8 | X9 | X10 |
|-----|----|--------|--------|---------|---------|---------|---------|---------|---------|---------|
| X1 | 1 | 0.0104 | 0.8858 | 0.0378 | -0.1221 | -0.1445 | -0.0439 | -0.0062 | -0.0107 | -0.0157 |
| X2 | | 1 | 0.0434 | 0.0052 | 0.1234 | 0.0457 | -0.0429 | -0.0443 | 0.1674 | 0.1196 |
| X3 | | | 1 | -0.0330 | -0.1521 | -0.1767 | -0.0477 | -0.0537 | -0.0344 | -0.0314 |
| X4 | | | | 1 | -0.1217 | -0.0400 | -0.1468 | 0.1636 | 0.0321 | 0.2438 |
| X5 | | | | | 1 | 0.1635 | -0.0479 | -0.0649 | 0.1742 | -0.0274 |
| X6 | | | | | | 1 | 0.2210 | -0.1298 | -0.0810 | 0.0829 |
| X7 | | | | | | | 1 | 0.0734 | -0.3143 | -0.0987 |
| X8 | | | | | | | | 1 | -0.2318 | 0.0640 |
| X9 | | | | | | | | | 1 | -0.0970 |
| X10 | | | | | | | | | | 1 |

Note: X1) slope, X2) aspect, X3) relief, X4) distance to drainage, X5) drainage density, X6) lithology, X7) distance to fault, X8) vegetation coverage, X9) landuse, distance to road.

9 factors including slope, slope aspect, fault distance, engineering rock formation, water system distance, water system density, vegetation coverage, land use type, and road distance. And use these factors as the impact factors of collapse susceptibility evaluation.

3.2. Calculate the Collapse Frequency Ratio of Each Factor

The statistical analysis of the collapse frequency of each factor (**Table 3**) shows

Table 3. Frequency ratio—spatial relationship between collapse and related factors.

| Factor | Class | No of pixels in domain | % of domain | No of collapse | % of collapse | Frequency ratio |
|-------------------|----------------------|------------------------|-------------|----------------|---------------|-----------------|
| slope | 0° - 7° | 1,073,644 | 0.26 | 80 | 0.13 | 0.51 |
| | 8° - 15° | 1,198,235 | 0.29 | 165 | 0.27 | 0.94 |
| | 16° - 25° | 1,003,687 | 0.24 | 189 | 0.31 | 1.29 |
| | 26° - 35° | 584,757 | 0.14 | 109 | 0.18 | 1.28 |
| | >35° | 342,937 | 0.08 | 70 | 0.11 | 1.40 |
| aspect | flat | 32,863 | 0.01 | 3 | 0.00 | 0.63 |
| | N | 642,052 | 0.15 | 67 | 0.11 | 0.72 |
| | NE | 692,751 | 0.16 | 60 | 0.10 | 0.59 |
| | E | 622,710 | 0.15 | 82 | 0.13 | 0.90 |
| | SE | 420,737 | 0.10 | 105 | 0.17 | 1.71 |
| | S | 291,204 | 0.07 | 79 | 0.13 | 1.86 |
| | SW | 343,071 | 0.08 | 64 | 0.10 | 1.28 |
| | W | 496,177 | 0.12 | 73 | 0.12 | 1.01 |
| Rock formation | NW | 661,695 | 0.16 | 80 | 0.13 | 0.83 |
| | γ | 6633 | 0.00 | 1 | 0.00 | 1.03 |
| | P | 148,296 | 0.04 | 9 | 0.01 | 0.42 |
| | D | 125,551 | 0.03 | 17 | 0.03 | 0.93 |
| | C | 525,137 | 0.13 | 87 | 0.14 | 1.13 |
| | T | 37,800 | 0.01 | 4 | 0.01 | 0.72 |
| | J | 1,437,427 | 0.34 | 310 | 0.51 | 1.48 |
| | K | 337,300 | 0.08 | 38 | 0.06 | 0.77 |
| | E-N | 407,080 | 0.10 | 16 | 0.03 | 0.27 |
| | Q ₃ pl-Q1 | 944,836 | 0.22 | 69 | 0.11 | 0.50 |
| Distance to fault | Q4 | 229,234 | 0.05 | 62 | 0.10 | 1.85 |
| | 0 - 1500 | 1,706,529 | 0.41 | 262 | 0.43 | 1.05 |
| | 1500 - 3000 | 969,084 | 0.23 | 164 | 0.27 | 1.16 |
| | 3000 - 4500 | 576,434 | 0.14 | 90 | 0.15 | 1.07 |

Continued

| | | | | | | |
|----------------------|-------------|-----------|------|------|------|------|
| | 4500 - 6000 | 314,183 | 0.07 | 40 | 0.07 | 0.87 |
| | >6000 | 637,030 | 0.15 | 57 | 0.09 | 0.61 |
| Distance to drainage | 0 - 400 | 1,347,761 | 0.32 | 462 | 0.75 | 2.35 |
| | 400 - 800 | 1,057,751 | 0.25 | 61 | 0.10 | 0.40 |
| | 800 - 1200 | 770,110 | 0.18 | 38 | 0.06 | 0.34 |
| | 1200 - 1600 | 493,007 | 0.12 | 26 | 0.04 | 0.36 |
| | 1600 - 2000 | 298,034 | 0.07 | 19 | 0.03 | 0.44 |
| | 2000 - 2400 | 152,031 | 0.04 | 1 | 0.00 | 0.05 |
| | > 2400 | 83,953 | 0.02 | 6 | 0.01 | 0.49 |
| | <0.9 | 340,394 | 0.08 | 28 | 0.05 | 0.56 |
| Drainage density | 0.9 - 1.1 | 1,467,727 | 0.35 | 303 | 0.49 | 1.42 |
| | 1.1 - 1.3 | 1,622,182 | 0.39 | 220 | 0.36 | 0.93 |
| | 1.3 - 1.5 | 535,987 | 0.13 | 51 | 0.08 | 0.65 |
| Vegetation coverage | >1.5 | 236,970 | 0.06 | 11 | 0.02 | 0.32 |
| | 0 - 10 | 52,106 | 0.01 | 18 | 0.03 | 2.37 |
| | 10 - 20 | 204,481 | 0.05 | 134 | 0.22 | 4.49 |
| | 20 - 50 | 1,342,133 | 0.32 | 250 | 0.41 | 1.28 |
| | 50 - 75 | 1,256,607 | 0.30 | 129 | 0.21 | 0.70 |
| | 75 - 100 | 1,347,933 | 0.32 | 82 | 0.13 | 0.42 |
| landuse | farmland | 76,034 | 0.02 | 0 | 0.00 | 0.00 |
| | forest | 465,553 | 0.11 | 45 | 0.08 | 0.68 |
| | grass | 715,834 | 0.17 | 125 | 0.21 | 1.23 |
| | water | 50,268 | 0.01 | 0 | 0.00 | 0.00 |
| | reservoir | 9289 | 0.00 | 0 | 0.00 | 0.00 |
| | tidal flat | 30,096 | 0.01 | 15 | 0.03 | 3.52 |
| | snow | 8361 | 0.00 | 0 | 0.00 | 0.00 |
| | buildup | 24,498 | 0.01 | 13 | 0.02 | 3.75 |
| | bare soil | 1,402,056 | 0.33 | 90 | 0.15 | 0.45 |
| | gravel | 138,930 | 0.03 | 45 | 0.08 | 2.29 |
| rock | 1,278,393 | 0.30 | 262 | 0.44 | 1.45 | |
| Distance to road | 0 - 500 | 1,244,095 | 0.30 | 488 | 0.80 | 2.69 |
| | 500 - 1000 | 993,747 | 0.24 | 37 | 0.06 | 0.26 |
| | 1000 - 1500 | 750,692 | 0.18 | 28 | 0.05 | 0.26 |
| | 1500 - 2000 | 511,891 | 0.12 | 25 | 0.04 | 0.33 |
| | 2000 - 2500 | 322,199 | 0.08 | 13 | 0.02 | 0.28 |
| | >2500 | 380,636 | 0.09 | 22 | 0.04 | 0.40 |

that the slope of collapse is also concentrated between 7° and 15°, with a total of 354 places, accounting for 57.75% of the total number of collapses, while the slope aspect does not affect the distribution of collapses, relatively uniform in all directions. The closer the collapse is to the fault, the greater the number of occurrences, with 42.74% occurring within 1500 m. The influence of lithology on the collapse is obvious, and 50% is concentrated in the layered hard conglomerate, sandstone, shale and coal rock areas. The distance between the water system and the collapse has a linear relationship. The closer to the water system, the easier it is to collapse. Collapses are more likely to occur in areas with vegetation coverage of 20% - 50%, accounting for 40.78% of the total number of collapses. The influence of the distance to the water system on the collapse is very obvious. There are 462 collapses within 400 m. The farther the distance is, the smaller the probability of occurrence is. There is no obvious correlation between the influence of the water system density on the collapse. Among the collapse types, grassland and tidal flats have a significant impact on landslides. The influence of tidal flats on collapse is closely related to the water system.

Using the frequency ratio (**Table 3**) and Equation (4), the LSI values were computed. The LSI values were reclassified to 4 grades by 7.5, 10, 13 (**Figure 2**). The LSI value is high, there is a higher susceptibility to collapses; a lower value indicates a lower susceptibility to collapses. low susceptibility zone (LSI = 4 - 7.5), covering area 584.04 km², only 3 collapses happened, and 0.39% of total collapses. Middle susceptibility zone (LSI = 7.5 - 10), covering area 1241.15 km², 35 collapses happened, and 5.66% of total collapses. High susceptibility zone (LSI = 10 - 13), covering area 751.95 km², 64 collapses happened, and 10.36% of total collapses. Extremely high susceptibility zone (LSI = 13 - 22), covering area 1206.34 km², 516 collapses happened, and 83.5% of total collapses.

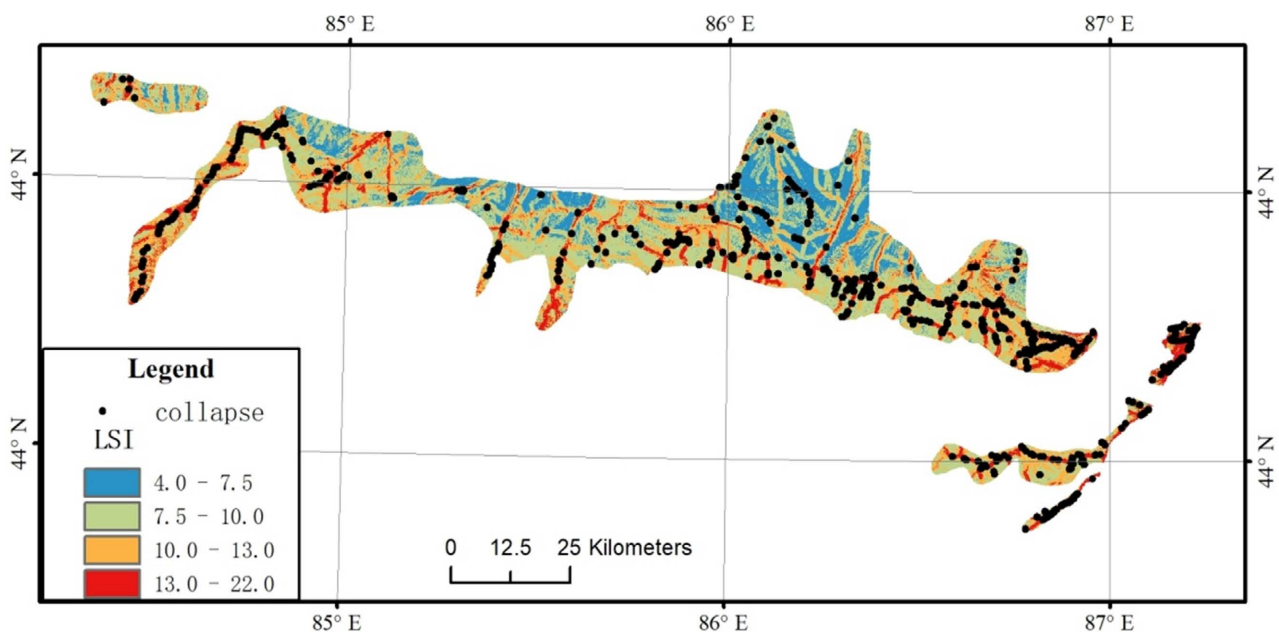


Figure 2. Collapse susceptibility index LSI spatial distribution map.

4. Discussion and Conclusion

Collapse is a geological disaster second only to landslides and occurs in large numbers every year. Using the GIS-based frequency method, the susceptibility to collapse was calculated and mapped, which was in good agreement with the actual landslide data. Collapse susceptibility results provide guidance for engineering construction.

In the evaluation process, the main problem encountered is that the scales of the collected data are different and come from different departments. How much will affect the final result, a correlation study is needed.

Conflicts of Interest

The authors declare no conflicts of interest regarding the publication of this paper.

References

- Bragagnolo, L., da Silva, R. V., & Grzybowski, J. M. V. (2020). Landslide Susceptibility Mapping with Landslide: A Free Open-Source GIS-Integrated Tool Based on Artificial Neural Networks. *Environmental Modelling & Software*, *123*, 104565. <https://doi.org/10.1016/j.envsoft.2019.104565>
- Fang, M., Zhang, J. L., & Xu, Z. (2011). Landslide Susceptibility Zoning Study in Lanzhou City Based on GIS and Logistic Regression Model. *Remote Sensing Technology and Application*, *26*, 845-854.
- He, S. S., Wang, J., & Wang, H. J. (2019). Real-Time Warning Test of Landslide and Debris Flow with a Statistical Model in Large Scale. *Transactions of Atmospheric Sciences*, *42*, 78-92.
- Huang, F., Zhang, J., Zhou, C., Wang, Y., Huang, J., & Zhu, L. (2020). A Deep Learning Algorithm Using a Fully Connected Sparse Auto Encoder Neural Network for Landslide Susceptibility Prediction. *Landslides*, *17*, 217-229. <https://doi.org/10.1007/s10346-019-01274-9>
- Intarawichian, N., & Dasananda, S. (2011). Frequency Ratio Model Based Landslide Susceptibility Mapping in Lower Mae Chaem Watershed, Northern Thailand. *Environmental Earth Science*, *64*, 2271-2285. <https://doi.org/10.1007/s12665-011-1055-3>
- Lee, S., & Lee, M.-J. (2006). Detecting Landslide Location Using KOMPSAT 1 and Its Application to Landslide-Susceptibility Mapping at the Gangneung Area, Korea. *Advances in Space Research*, *38*, 2261-2271. <https://doi.org/10.1016/j.asr.2006.03.036>
- Lee, S., & Talib, J. A. (2005). Probabilistic Landslide Susceptibility and Factor Effect Analysis. *Environmental Geology*, *47*, 982-990. <https://doi.org/10.1007/s00254-005-1228-z>
- Li, W. Y., & Wang, X. L. (2020). Application and Comparison of Frequency Ratio and Information Value Model for Evaluating Landslide Susceptibility of Loess Gully Region. *Journal of Natural Disasters*, *29*, 213-220.
- Li, L. P., Lan, H. X., Guo, C. B., et al. (2017). A Modified Frequency Ratio Method for Landslide Susceptibility Assessment. *Landslides*, *14*, 727-741. <https://doi.org/10.1007/s10346-016-0771-x>
- Li, Y., Sheng, Y., Chai, B., Zhang, W., Zhang, T., & Wang, J. (2020). Collapse Susceptibility Assessment Using a Support Vector Machine Compared with Back-Propagation and Radial Basis Function Neural Networks. *Geomatics, Natural Hazards and Risk*, *11*,

510-534. <https://doi.org/10.1080/19475705.2020.1734101>

Polykretis, C., & Chalkias, C. (2018). Comparison and Evaluation of Landslide Susceptibility Maps Obtained from Weight of Evidence, Logistic Regression, and Artificial Neural Network Models. *Natural Hazards*, *93*, 249-274.

<https://doi.org/10.1007/s11069-018-3299-7>

Poudyal, C. P., Chang, C., Oh, H. J., et al. (2010). Landslide Susceptibility Maps Comparing Frequency Ratio and Artificial Neural Networks: A Case Study from the Nepal Himalaya. *Environmental Earth Sciences*, *61*, 1049-1064.

<https://doi.org/10.1007/s12665-009-0426-5>

Shi, H., Deng, N. D., & Zhou, Y. (2021). Evaluation of Collapse Susceptibility Based on Random Forest Weighted Analytic Hierarchy Process. *Science Technology and Engineering*, *21*, 10613-10619.

Farr, T. G., Rosen, P. A., Caro, E., et al. (2007). The Shuttle Radar Topography Mission. *Reviews of Geophysics*, *45*, RG2004. <https://doi.org/10.1029/2005RG000183>

Van Den Eeckhaut, M., Hervas, J., Jaedicke, C., et al. (2012). Statistical Modeling of Europe-Wide Landslide Susceptibility Using Limited Landslide Inventory Data. *Landslides*, *9*, 357-369. <https://doi.org/10.1007/s10346-011-0299-z>

Xing, X. F., Wu, C. L., Li, J. H., et al. (2021). Susceptibility Assessment for Rainfall-Induced Landslides Using a Revised Logistic Regression Method. *Natural Hazards*, *106*, 97-117.

<https://doi.org/10.1007/s11069-020-04452-4>

Xu, X. H. (2010). Approach Study of Landslides Susceptibility Mapping Using Logistic Regression Model. *Journal of Rail Way Science and Engineering*, *7*, 87-91.